

# Study on high precision single-pole magnetic encoder based on error analysis and compensation method

Yuyuan Liu\*, Mingjiang Wang

School of Electronics and Information Engineering, Harbin Institute of Technology (Shenzhen), Shenzhen, 518000, China

\*Corresponding author's e-mail: 13568040689@163.com

**Abstract.** This paper introduces the basic principle of single-pole magnetic encoder and its application in industrial field, and analyses three main sources of errors of single-pole magnetic encoder, including unequal amplitude of signal, non-orthogonal phase of input signal, and high order harmonic in input signal. According to the principle of the decoding algorithm of the magnetic encoder, the paper pushed out mathematical expression of each kind of error, and developed the corresponding compensation measures according to these expressions. Finally, we using the STM3232F103 microprocessor as the carrying platform of the algorithm and the 16-bit precision servo motor system as a reference, verified the validity of the error compensation algorithm.

## 1. Introduction

The position sensor plays a central role in the industrial servo system. The control accuracy of the servo control system depends largely on the position feedback accuracy and stability of the encoder. Position sensors currently used mainly include the magnetic encoder and optical encoder.

Optical encoder is the most widely used position sensor in industry due to its mature technology and high precision. However optical encoders are unable to work in extreme conditions such as such as oil, moisture, dust, and mechanical vibration. Besides its structural principle makes it difficult to maintain a small volume when optical encoder improving its angular resolution [1-2].

Compared with optical encoders, magnetic encoders have good anti-vibration performance and are not affected by dust and haze conditions. Magnetic encoders are divided into single-pole magnetic encoders and multi-pole magnetic encoders. In order to improve the accuracy, multipole magnetic encoders usually use more magnetic poles, but it also leads to the problems of complicated structure and large volume of encoders, and the output accuracy of encoders is affected by the high order harmonic in signals [3-4]. Single-pole magnetic encoder is small in size and compact in structure, which can meet the needs of miniaturization and lightweight applications. However, due to the limitations of processing technology and assembly technology, the actual air gap magnetic field distribution state has different degrees of errors compared with the ideal state, which cannot reach the ideal state, resulting in generally low resolution of magnetic encoders [5]. In order to improve the accuracy of magnetic encoders, many researchers have proposed different ways of improvement. Calibration table lookup [6] is a common magnetic encoder decoding algorithm, which has the characteristics of fast decoding speed and low algorithm complexity. However, the lookup table method needs to store a large amount of calibration information in ROM and occupies a large amount of memory resources. Besides the accuracy of the algorithm is limited by the calibration accuracy. The magnetic encoder decoding algorithm based on arctangent method [7-8] is easy to implement in both hardware and software, but the assembly error will



lead to signal distortion, so the Angle value calculated by the traditional arctangent algorithm is not accurate. In [9], the error compensation table method is proposed to solve the errors caused by mechanical installation, and the crossover interval linear interpolation method is proposed to reduce the interference of noise signals. The above methods have their own advantages in decoding speed, resource consumption, mechanical installation and other dimensions. However, the error of magnetic encoder is not analyzed systematically, and the method of Angle solving is inefficient.

In this paper, we analyze three main error sources, amplitude imbalance, non-orthogonal phase and high order harmonic in signals which affect the decoding accuracy and designed the corresponding error compensation algorithm.

The rest of this paper is organized as follows. Section 2 introduces the basic structure of magnetic encoder and deduces the formula of different kinds of errors of magnetic encoder. Section 3 proposes three kinds of error compensation schemes for different kinds of errors. We will present our experimental data in Section 4. Section 5 concludes this paper.

## 2. error analysis of single-pole magnetic encoder

### 2.1. Structure of single-pole magnetic encoder

The structure of single-pole magnetic encoder can be shown in figure 1. After the air gap magnetic field of the integrated hall encoder is established, the linear hall element outputs two cosine voltage signals with orthogonal phase under ideal conditions which can be expressed as:

$$V_a = V_0 + A \sin \theta \quad (1)$$

$$V_b = V_0 + A \cos \theta \quad (2)$$

Where  $\theta$  is the actual physical position of the motor rotor and  $V_0$  is the dc component which is easy to calculate. The absolute physical position and rotation speed of the rotor can be obtained by using arctangent operation with the two orthogonal signals.

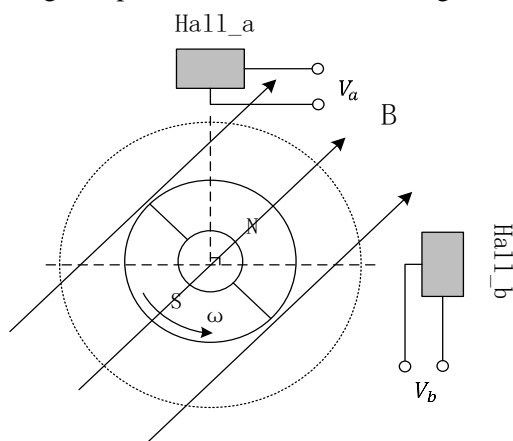


Figure 1. Structure of the single-pole magnetic encoder

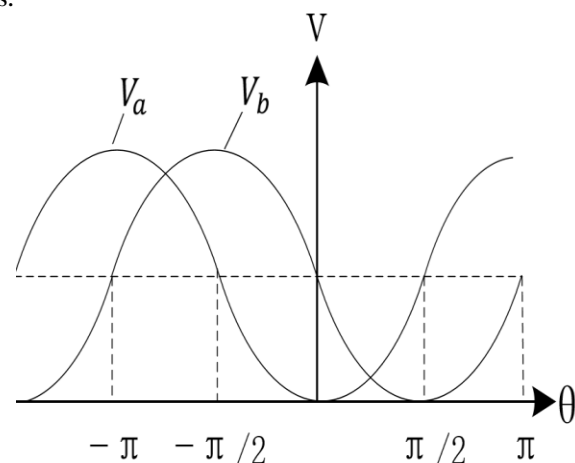


Figure 2. Orthogonal voltage outputs of the hall.

The error of original voltage signal output by magnetic encoder is mainly caused by the installation deviation of hall element and the low quality of air-gap magnetic field. In addition, also related to electrical, temperature and aging factors. The errors of magnetic encoder mainly include: amplitude imbalance, non-orthogonal phase and high order harmonic in signals. The specific analysis is as follows:

### 2.2. Errors caused by amplitude imbalance

The input voltage can be expressed as:

$$V_a = V_0 + A \sin \theta \quad (3)$$

$$V_b = V_0 + (1 + \alpha)A \cos \theta \quad (4)$$

The formula for calculating the Angle can be expressed as:

$$\varphi = \tan^{-1}\left(\frac{A \sin \theta}{(1+\alpha)A \cos \theta}\right) \quad (5)$$

The error is as follows:

$$\varepsilon = \theta - \varphi = \theta - \tan^{-1}\left(\frac{\tan \theta}{1+\alpha}\right) \quad (6)$$

transforming the equation (6):

$$\tan \varepsilon = \tan\left(\theta - \tan^{-1}\left(\frac{\tan \theta}{1+\alpha}\right)\right) = \frac{\tan \theta - \frac{\tan \theta}{1+\alpha}}{1 + \tan \theta \frac{\tan \theta}{1+\alpha}} = \frac{\alpha}{2} \sin 2\theta \frac{1}{\alpha \cos^2 \theta + 1} \quad (7)$$

In general,  $\varepsilon$  and  $\alpha$  is small, in this case  $\tan \varepsilon \approx \varepsilon$ ,  $1 + \alpha \cos^2 \theta \approx 1$ , the equation (7) can be simplified as:

$$\varepsilon \approx \frac{\alpha}{2} \sin 2\theta \quad (8)$$

### 2.3. Errors caused by non-orthogonal phase

Suppose the phase difference of two voltage signals is  $\beta$ , the input voltage can be expressed as:

$$V_a = V_0 + A \sin \theta \quad (9)$$

$$V_b = V_0 + A \cos(\theta + \beta) \quad (10)$$

The formula for calculating the Angle can be expressed as:

$$\varphi = \tan^{-1}\left(\frac{\sin \theta}{\cos(\theta + \beta)}\right) \quad (11)$$

The error is as follows:

$$\varepsilon = \theta - \varphi = \theta - \tan^{-1}\left(\frac{\sin \theta}{\cos(\theta + \beta)}\right) \quad (12)$$

transforming the equation (12):

$$\tan \varepsilon = \tan\left(\theta - \tan^{-1}\left(\frac{\sin \theta}{\cos(\theta + \beta)}\right)\right) = \frac{\tan \theta - \frac{\sin \theta}{\cos(\theta + \beta)}}{1 + \tan \theta \frac{\sin \theta}{\cos(\theta + \beta)}} = \frac{\sin \theta \cos \theta \cos \beta - \sin^2 \theta \sin \beta - \sin \theta \cos \theta}{\cos(\theta + \beta) \cos \theta + \sin^2 \theta} \quad (13)$$

In general,  $\varepsilon$  and  $\beta$  is small, in this case  $\tan \varepsilon \approx \varepsilon$ ,  $\sin \beta \approx \beta$ ,  $\cos \beta \approx 1$ ,  $\cos(\theta + \beta) \cos \beta + \sin^2 \theta \approx 1$  the equation (13) can be simplified as:

$$\varepsilon \approx -\frac{\beta}{2}(1 - \cos 2\theta) \quad (14)$$

### 2.4. Errors caused by high order harmonic

The Fourier series form of the input vector expression is shown in the formula:

$$V_{in} = V(K_0 + \sum_{n=1}^{\infty} K_n \cos(n\theta)) + jV(K_0 + \sum_{n=1}^{\infty} K_n \sin(n\theta)) = V(\sqrt{2}K_0 e^{j\frac{\pi}{4}} + \sum_{n=1}^{\infty} K_n e^{jn\theta}) \quad (15)$$

The  $K_1$  is equal to 1,  $K_0, K_2, K_3, \dots, K_N$  is much smaller than 1, the Angle can be expressed as:

$$\varphi = \tan^{-1}\left(\frac{K_0 + \sum_{n=1}^{\infty} K_n \sin(n\theta)}{K_0 + \sum_{n=1}^{\infty} K_n \cos(n\theta)}\right) \quad (16)$$

The error is as follows:

$$\begin{aligned} \tan \varepsilon &= \tan \left( \theta - \tan^{-1} \left( \frac{K_0 + \sum_{n=1}^{\infty} K_n \sin(n\theta)}{K_0 + \sum_{n=1}^{\infty} K_n \cos(n\theta)} \right) \right) = \frac{\tan \theta - \frac{K_0 + \sum_{n=1}^{\infty} K_n \sin(n\theta)}{K_0 + \sum_{n=1}^{\infty} K_n \cos(n\theta)}}{1 + \tan \theta \frac{K_0 + \sum_{n=1}^{\infty} K_n \sin(n\theta)}{K_0 + \sum_{n=1}^{\infty} K_n \cos(n\theta)}} \\ &= \frac{\sin \theta (K_0 + \sum_{n=1}^{\infty} K_n \cos(n\theta)) - \cos \theta (K_0 + \sum_{n=1}^{\infty} K_n \sin(n\theta))}{\cos \theta (K_0 + \sum_{n=1}^{\infty} K_n \cos(n\theta)) + \sin \theta (K_0 + \sum_{n=1}^{\infty} K_n \sin(n\theta))} = \\ &= \frac{K_0 (\sin \theta - \cos \theta) + \sum_{n=2}^{\infty} K_n (\cos(n\theta) \sin \theta - \sin(n\theta) \cos \theta)}{K_0 (\sin \theta - \cos \theta) + 1 + \sum_{n=2}^{\infty} K_n (\cos(n\theta) \sin \theta - \sin(n\theta) \cos \theta)} = \frac{-\sqrt{2} K_0 \cos\left(\theta + \frac{\pi}{4}\right) - \sum_{n=2}^{\infty} K_n \sin((n-1)\theta)}{\sqrt{2} K_0 \sin\left(\theta + \frac{\pi}{4}\right) + 1 + \sum_{n=2}^{\infty} K_n \cos((n-1)\theta)} \quad (17) \end{aligned}$$

Due to each harmonic coefficient  $K_0, K_2, K_3, \dots, K_N$  is much smaller than 1,  $\tan \varepsilon \approx \varepsilon$ , the denominator can be approximated as 1, the equation (17) can be simplified as:

$$\varepsilon \approx -\sqrt{2} K_0 \cos\left(\theta + \frac{\pi}{4}\right) - \sum_{n=2}^{\infty} K_n \sin((n-1)\theta) \quad (18)$$

### 3. compensation method of the error

In the previous chapter, we made a detailed analysis of the three main error sources of the magnetic encoder and obtained the mathematical expressions of each error. In this chapter, we given three different compensation schemes for the above three different types of errors. Concrete analysis is as follows:

#### 3.1. Filtering processing

We use a low pass filter to process the higher harmonics in the signal. To be specific we use a two-stage filtering method, first using median filtering and then using mean filtering. The median filter has a good filtering effect on the salt and pepper noise, and the mean filtering can filter the Gaussian noise in the signal.

#### 3.2. Amplitude normalization and phase orthogonalization algorithm

In order to solve the problem of unequal amplitude of input signal, we use equation (19) to normalize the input data.

$$V_{out} = \frac{A_{out}(V_{in} - V_{min})}{A_{in}} - \frac{A_{out}}{2} \quad (19)$$

Where  $V_{in}$  is the original signal,  $A_{in}$  is amplitude of the original signal, and  $A_{out}$  is the amplitude of the signal after normalization.  $V_{min}$  is the minimum values of the original signal.

According to equation (14), As long as we can figure out the phase difference  $\beta$  between the two signals, We can calculate the error caused by the non-orthogonal phase according to equation (14).

So the question is, how do you figure out the amplitude of the original signal and the phase difference  $\beta$  between the two signals. In this design, we use the discrete Fourier transform (DFT) to solve the amplitude and phase information of the input signal.

The discrete Fourier transform (DFT) can transform a signal into the frequency domain. Some signals are hard to see in the time domain, but when you go to the frequency domain, it's easy to see. An analog signal, when sampled by an ADC, becomes a digital signal. The sampling theorem tells us that the sampling frequency is greater than twice the signal frequency. After sampling the digital signal, FFT transformation can be done. There are N sampling points in total. After DFT, there are N points can be obtained. For the convenience of DFT operation, N usually takes 2 to the integer power.

According to the basic theory of discrete Fourier transform, if we suppose the sampling frequency is  $F_s$  and the sampling number is N, After DFT, the frequency expressed by a certain point n (n starts from 1) is:  $F_n = \frac{(n-1)F_s}{N}$ , The magnitude of the point divided by  $\frac{N}{2}$  is the magnitude of the signal at the given frequency (For a dc signal it's divided by N). The phase of the point is the phase of the signal at the corresponding frequency.

The input signal can be expressed as:

$$X(n) = A_{dc} + A \cos(2\pi f_0 t(n) + \varphi)$$

In this design, we set the motor rotation frequency  $f_0$  as 10hz, DC signal amplitude  $A_{dc}$  as 3, AC signal amplitude  $A$  as 2. The sampling frequency is set to 64hz and the number of sampling points is 64. Figure 3 shows the time-domain sampling of the cosine signal. Figure 4 shows the relationship between the amplitude and frequency of the signal after the discrete Fourier transform.

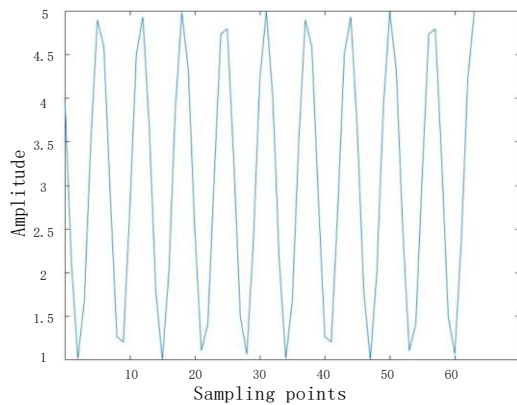


Figure 3. The input sampling signal.

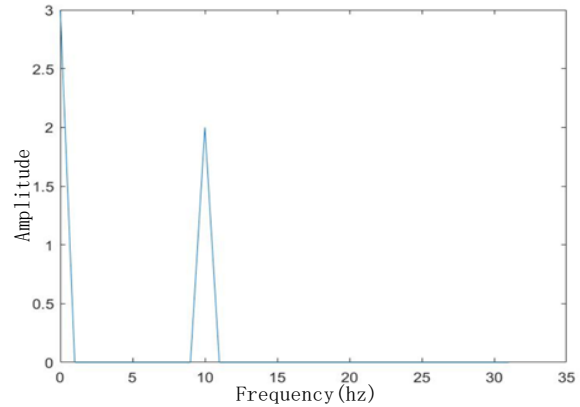


Figure 4. Amplitude-frequency curve.

Since the discrete Fourier transform can accurately calculate the amplitude and phase information of the input signal, according to equation (14), the error caused by non-orthogonal phase can be compensated.

#### 4. Experiment and Error Validation

In order to verify the accuracy of the algorithm, we took 16-bit precision servo motor system as a reference, and STM32F103 microprocessor as the platform for the algorithm. We send the angle data of magnetic encoder module to PC for simple processing through RS485 serial port communication module. The accuracy verification system of the magnetic encoder is shown in figure 12. In the experiment, we test the traditional decoding algorithm and the decoding algorithm with error compensation. Figure 6 shows the error curves of the two algorithms between 0 and 360 degrees. As shown in figure 6, the performance of the magnetic encoder is significantly improved after adding the error compensation algorithm. The maximum error of the magnetic encoder is within  $0.5^\circ$

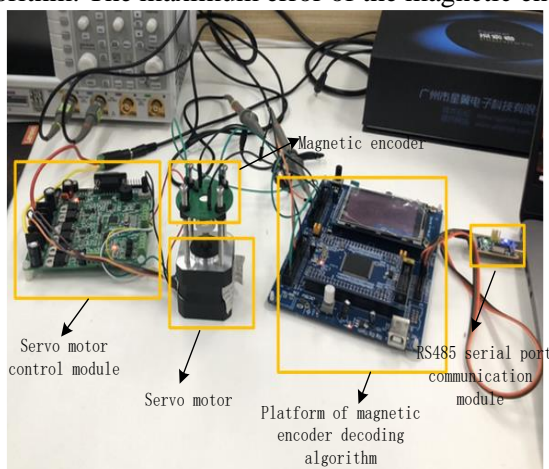


Figure 5. The magnetic encoder error validation experimental platform.

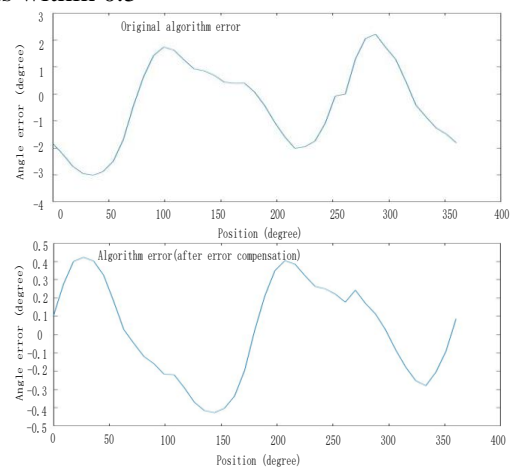


Figure 6. The accuracy curve of the original decoding algorithm and the decoding algorithm with error compensation.

## 5. Conclusion

Magnetic encoders are widely used in industrial servo control systems. In this paper, various error sources in the decoding algorithm of magnetic encoders are analyzed, including amplitude unbalance, non-orthogonal phase, harmonic and its influence on accuracy. More importantly, an Angle compensation algorithm is proposed to correct the Angle error and maximize the accuracy of the magnetic encoder module. Finally, we use a 16-bit precision servo motor system as a reference standard to verify the accuracy of the compensation algorithm. Experimental results show that this method can effectively eliminate errors and improve the accuracy of the algorithm.

## References

- [1] Y Li, T Endo, K Hane 2003 Projection type micro optical encoder based on MEMS technology *Guang Xue Xue Bao.* **23(8)** 1005-1007.
- [2] Johannes 2003 An international length comparison at an industrial level using photoelectric incremental encoder as transfer standard *Precision Engineering.* **27** 151-156.
- [3] Shi Y, Liu Y L, Zhang H W 2005 Model of MR sensor with slant multiphase filtering *Piezoelectrics and Acousto-optics.* **7(1)** 74-76.
- [4] Chiriac H, Marinescu C S, Marinescu M 2005 Hard and soft amorphous magnetic materials based micro rotary encoder *Materials Science Forum.* **37(4)** 361-364.
- [5] Lin Q, Li T, Zhou Z 2011 Error analysis and compensation of the orthogonal magnetic encoder. In: International Conference on Instrumentation. Beijing. pp. 1-4.
- [6] HAO S H, LIU Y, LIU J. 2006 Design of single pair pole magnetic encoder based on looking-up table *Proceedings of the CSEE.* **26(19)** 165-167.
- [7] Hu J, Zou J, Xu F, Li Y and Fu Y 2012 An improved PMSM rotor position sensor based on linear hall sensors *IEEE Trans. Mag.* **48(11)** 3591–3594.
- [8] Benammar M, Khattab A, Saleh S, Bensaali F, and Touati F 2017 A sinusoidal encoder-to-digital converter based on an improved tangent method *IEEE Sens. J.* **17(16)** 5169–5179.
- [9] Wang L, Li P, Qiao Y. 2017 Study on high precision magnetic encoder based on the arctangent cross-intervals tabulation method[J] *Australian Journal of Electrical and Electronics Engineering* **20** 1-7.